HEFAT2014
10th International Conference on Heat Transfer, Fluid Mechanics and Thermodynamics
14 – 16 July 2014
Orlando, Florida

NUMERICAL SIMULATION ON DRYING PROCESS OF AN INKJET DROPLET USING LAGRANGIAN FEM

Fukai J.*, Kubo K., Tanigawa T. and Nakaso K.
*Author for correspondence
Department of Chemical Engineering,
Kyushu University, Japan
E-mail: jfukai@chem-eng.kyushu-u.ac.jp

ABSTRACT

A mathematical model is proposed to describe the fluid dynamics, mass and heat transfer in a solution droplet evaporating on a flat surface during drying process. A decrease of droplet volume due to evaporation of a solvent, evaporation latent heat generated on the free surface, and an increase of a solute on the free surface are considered in the model. Governing equations are numerical solved using a finite element method. A Lagrangian method is applied to predict the deformation of an evaporating droplet. Firstly, the outward flow caused during self-pinning of the contact line are examined under an ideal condition. The calculated velocities agree well with calculated results using a one-dimensional model. Secondly, the drying process of a polystyrene/anisole solution droplet with the equivalent diameter of 20 μm are estimated. The migration of the solute at the contact line is found to be finished by the instant when a thin liquid film with a low solute concentration are still remained at the center part. As a result, a ring structure develops on the periphery of the dried film. Lastly, the effect of fluid viscosity is investigated. A high viscosity essentially decreases the fluid velocity, resulting in vanishing the ring structure. The effect of viscosity on the configuration of the film agrees with empirical results.

INTRODUCTION

Inkjet methods are expected to be an alternative process of vacuum evaporation methods for fabricating electric device such as organic EL display, organic TFT, display filters etc. A basic process of inkjet method is that solution or suspension droplets depositing on a substrate are dried, to form thin solid films. The most industrial applications require forming flat shape. However, it is not easy to make such a flat film: in general, a ring structure develops on the periphery of the film due to solute/particle transport toward the periphery. Flat shapes of thin films are empirically achieved on the industries by prepare boiling point of solvent, wettability and configuration of substrate surface, drying conditions and several operation parameters. However, theoretical studies on drying process of inkjet droplet have not been fully developed yet.

As numerical studies, the equations of continuity and momentum in the cylindrical coordinate system were numerically solved to discuss the fluid dynamics in droplets [1-2]. In addition, the effect of thermal Marangoni forces on the fluid dynamics was investigated numerically [2-2]. Hu *et al.*[5] reported the thermal Marangoni effect on local particles density in droplets. The fluid dynamics in a colloid nanoliter droplet was reported in details by Bhardwaj *et al.* [6]. Most of the numerical studies thus focused on the thermal Marangoni. In contrary, our research group has been studying the solutal Marangoni effect [7-8].

In this study, a mathematical model is proposed to predict not only the fluid dynamics but also a formed thin film shape. The model is numerically solved, to investigate the drying process of polystyrene/anisole solution droplet. The effect of viscosity is moreover discussed.

NOMENCLATURE

c_A	= solute concentration	[kg-solute/ kg-solvent]
C_p	= specific heat	[J/ (kg・K)]
d_0	= Initial droplet diameter	[m]
D_{AB}	= diffusion coefficient	[m^2/ s]
k	= thermal conductivity	[W/ (m・K)]
L	= evaporation latent heat	[J/ kg]
m''	= evaporation rate	[kg/ (m^2・s)]
$\boldsymbol{n}$	= unit vector normal to the free surface	[m]
p	= pressure	[Pa]
r	= radial distance	[m]
R	= r/ d_0	[-]
t	= time	[s]
T	= temperature	[K]
$\boldsymbol{u}$	= velocity vector	[m/ s]
V	= volume	[m^3]
z	= axial distance	[m]
Z	= z/ d_0	[-]
μ	= viscosity	[Pa・s]
$\boldsymbol{\pi}$	= stress tensor	[Pa]
ρ	= density	[kg/ m^3]

σ = surface tension [N/ m]
ϕ_c = contact angle [rad]

<Subscript>
0 = initial
A = solution
B = solvent
c = contact line
f = surface
l = liquid
w = substrate

MATHEMATICAL MODEL

Governing equations

Fig. 1 shows a schematic illustration of a computational domain, which is consists of a sessile droplet and substrate. On two-dimensional axis symmetric coordinate system, the equations of continuity, motion, solute mass and energy are given by Eqs. (1) - (4).

Equation of continuity:

$$\nabla \cdot \boldsymbol{u} = 0 \tag{1}$$

Equation of motion:

$$\rho_l \frac{D\boldsymbol{u}}{Dt} = -\nabla p + \nabla \cdot \mu_l \{\nabla \boldsymbol{u} + (\nabla \boldsymbol{u})^T\} \tag{2}$$

Equation of solute mass:

$$\frac{Dc_A}{Dt} = \nabla \cdot D_{AB} \nabla c_A \tag{3}$$

Equation of energy:

$$\rho_i C_{pi} \frac{DT_i}{Dt} = \nabla \cdot k_i \nabla T_i \ \text{(i=}l\text{, w)} \tag{4}$$

The initial conditions are given by

$$\boldsymbol{u} = 0,\ p = p_0,\ T_l = T_w = T_0,\ c_A = c_{A0} \tag{5}$$

As for boundary conditions, no-slip condition, the continuities of temperatures and heat fluxes, and no mass flux normal to the interface are given on the solid/liquid interface. The boundary conditions on the free surface are given by Eqs. (6) - (8):

$$\boldsymbol{\pi} \cdot \boldsymbol{n} + 2\sigma K \boldsymbol{n} = \nabla_s \sigma \begin{pmatrix} n_z \\ n_r \end{pmatrix} \tag{6}$$

$$-D_{AB} \frac{\partial c_A}{\partial n} = \frac{m''}{\rho_B} c_A \tag{7}$$

$$-k_l \frac{\partial T_l}{\partial n} = h(T_l - T_\infty) + m'' L \tag{8}$$

Thermal and solutal Marangoni forces are considered in Eq. (6). Condense of solute due to evaporation is considered in Eq. (7). Evaporation latent heat is considered in Eq. (8). The local evaporation rate *m*" is given by the model reported by H. Hu and R. G. Larson [9].

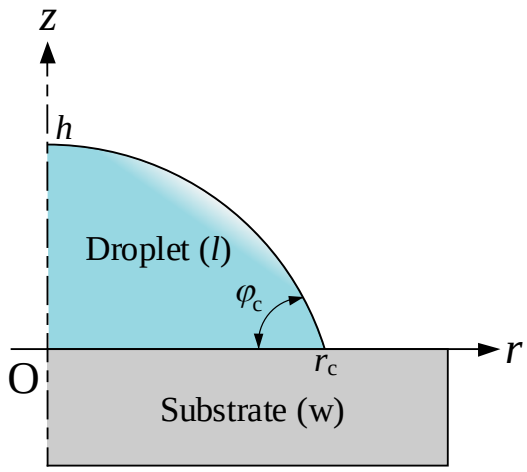

Fig. 1 Computational domain.

The governing equations are discretized using finite element method, and numerically solved. The algorism on the basis of a Lagrangian finite element method [11] was used.

Physical properties

Polystyrene/anisole solution was chosen in the calculation. Physical properties of anisole are shown in **Table 1**. The viscosity and surface tension of the solution were given as functions of solute concentration on the basis of the measured values [7], as shown in **Fig.2**. The measured values were obtained in the range of solute concentration $c_A < 0.2$ kg/ kg. To avoid the risk that unrealistic values are evaluated by extrapolations in the calculations, the maximum values were set at those for $c_A = 0.2$ kg/ kg. The temperature dependence of these properties can be neglected because isothermal system can be assumed in room temperature [7]. Mass diffusion coefficient D_{AB} was estimated using Wilke-Chang's equation [10]. The other physical properties were cited from physical properties handbooks, and assumed constants.

Table 1. Physical properties of anisole.

Boiling point [K]	Saturated vapor pressure [Pa]	Surface tension [mN/ m]	Viscosity [mPa·s]	Density [g/cm^3]
426.8	472	34.6	0.984	0.989

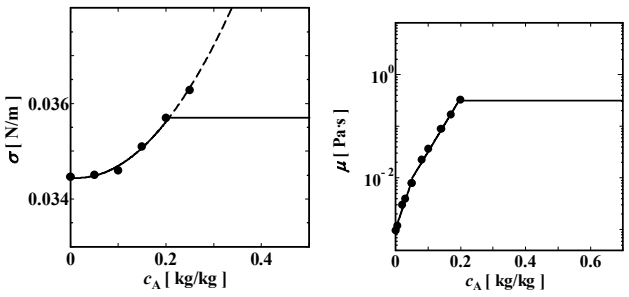

Fig. 2 Dependence of surface tension and viscosity on solute concentration.

RESULTS

Lateral outward flow during self-pinning

Deegan *et al.* [4] reported that evaporation of solvent derives a lateral outward flow in a deposited droplet, resulting in the migration of solute on the periphery of the droplet. To discuss the dry process of the droplet, numerical simulations have to predict this lateral outward flow. To confirm this issue, all physical properties were assumed to be at constant in the calculations. **Fig. 3** shows a typical result for velocity vector at the initial stage. The fluid is found to flow toward the contact line. The average velocities of the vertical cross section was calculated and plotted in **Fig. 4**. The initial droplet diameter is 20 μm. The initial contact angle is 30˚. Theoretical result was calculated from one-dimensional mass conservation equation of fluid in the *r*-direction under the assumption that the free surface maintains a part of sphere [12]. The calculated average velocities agree well with the theoretical ones.

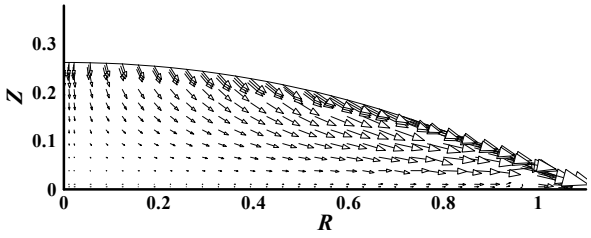

Fig. 3 Calculated flow velocity at the initial stage. (ϕ_c=30 ˚)

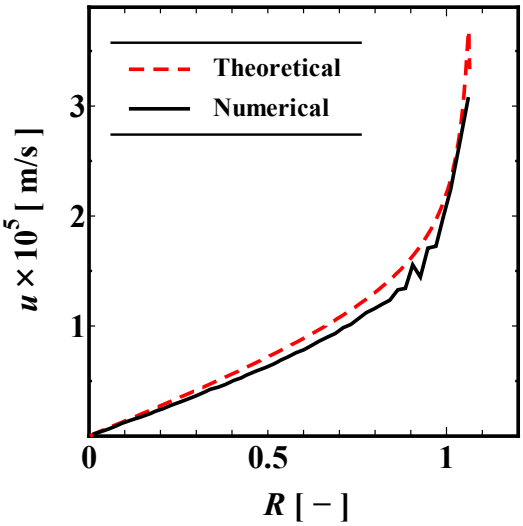

Fig. 4 The profile of the average velocity in the *r*-direction. (ϕ_c= 30 ˚)

Time variation of the droplet volume

There is very few quantities which can be compared to the experimental. Droplet volume is one of them. **Fig. 5** shows the time variation of the calculated droplet volume. The calculated droplet decreases due to evaporation, and agree well with the experiments.

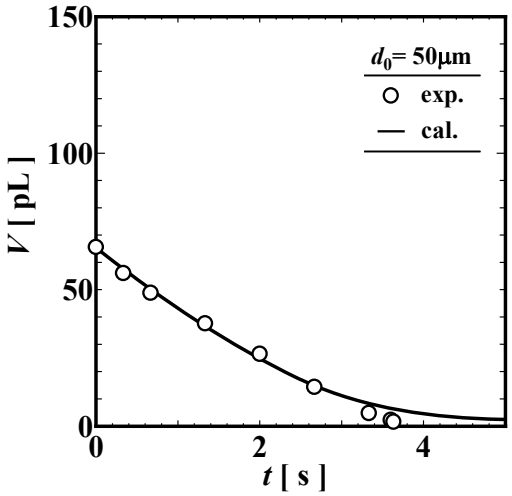

Fig. 5 Time variation of droplet volume.

A typical result of dry process

The calculations were performed for the initial contact angle ϕ_{c0} = 30 ˚, the initial equivalent diameter of the droplet d_0 = 20 μm, the initial solute concentration c_A = 0.01, the initial temperatures of the droplet and the substrate T = 298 K. The evaporation rate was set as a hundred times as large as the theoretical in the calculation. This is because we have not solved the technical problem on long computation time: that is, it took a week for the calculation to advance until the droplet almost dried. On the present assumption, the calculations were finished in a day using PC used here.

Figs. 6 shows the time variations of isothermal contours. V/V_0 represents the volume ratio of the instantaneous time to the initial. The temperature decreases from the bottom to the top because of evaporation of solvent. The temperature profile early develops, whose shape will not change. If comparing the calculated profiles with velocity fields (**Figs. 7**), the heat flows in the droplet is found to be dominated by heat conduction rather than convection.

Figs. 7 show the time variation of isoconcentration contours of solute (left side) and velocity vectors (right side). In **Fig. 7a**, the solute concentration c_A is obviously higher on the periphery of the liquid films. A thin solid film ($c_A \approx 1$) already appears on the periphery. At V/V_0= 0.2704 (**Fig. 7c**), a drastic concentration gradient is still developed. The liquid film at the center continues evaporating (**Fig. 7d**), and finally forms a thin film at the center (**Fig. 7e**). It is obvious that the thickness at the periphery is much thicker than that at center. This suggests that migration of the solute has caused at V/V_0= 0.2704 (**Fig. 7d**). The fluid velocities are directed outwards on the whole, decreasing from the periphery because of high viscosity.

Fig. 7d shows the ring structure develops under this condition. The experimental film photograph and configuration profile of the cross section are shown in **Fig. 8**. The experimental conditions are similar to the calculation condition. The calculated configuration has characteristics of the experimental films.

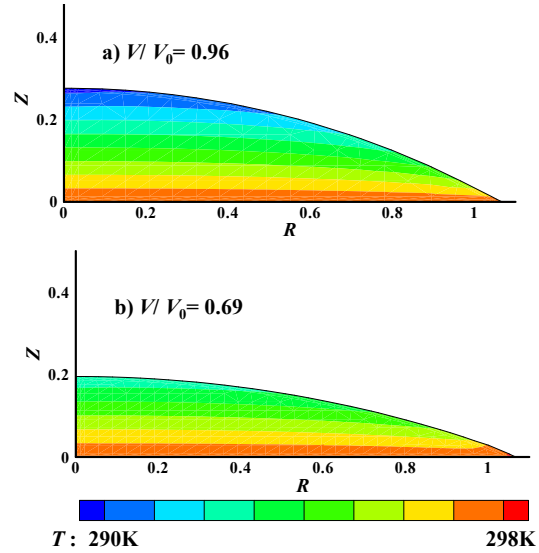

Figs. 6 Isothermal contours

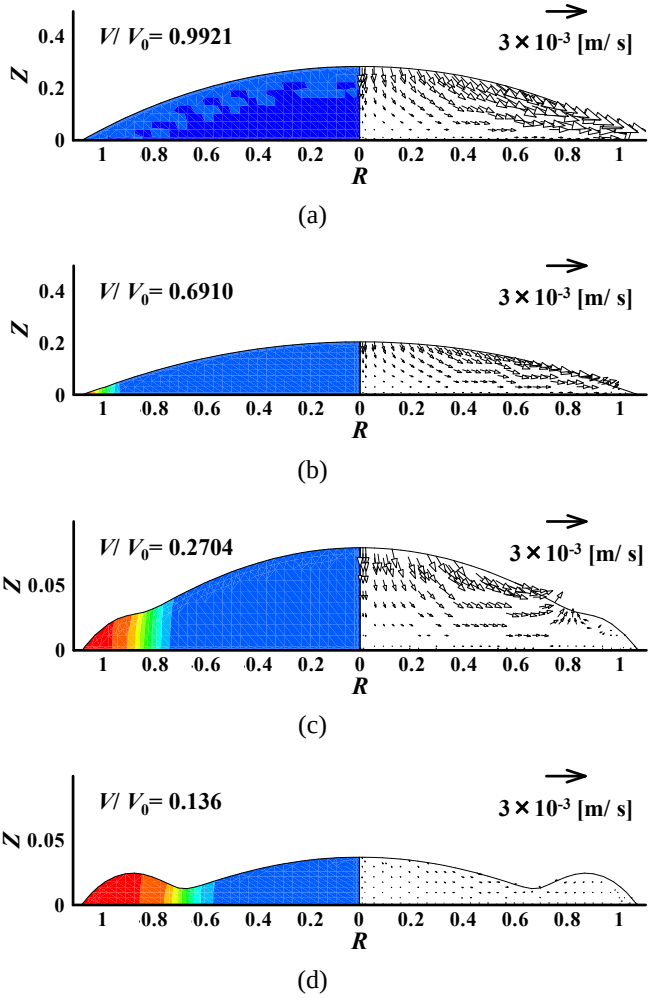

(a)

(b)

(c)

(d)

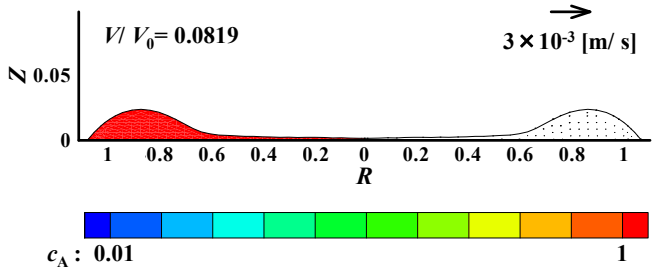

(e)

Figs. 7 Isoconcentration contours (left side) and velocity vectors (right side)

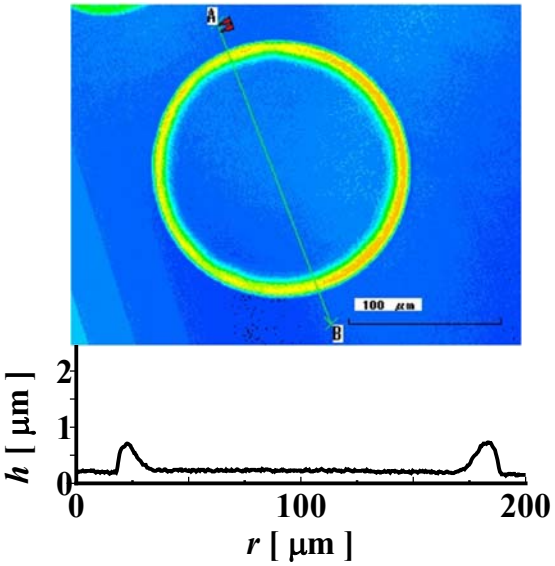

Fig. 8 Thin solid film from polystyrene/anisole solution droplet (c_{A0}= 0.03 kg/ kg)

Effect of outward flows on film configuration

The lateral flow shown in **Fig. 3** and **Fig. 4**, is known to be one of reasons for migration of solute near the contact line. To confirm this issue, the fluid viscosity was assumed to be a hundred times as large as that of the aforementioned calculation.

The effects of viscosity on the average velocity of lateral flow are shown in **Fig. 9**. The velocity certainly reduces as the viscosity increases. The formed thin film is nearly flat as shown in **Fig. 10**. This result supports that magnitude of fluid velocity essentially affects the film configuration.

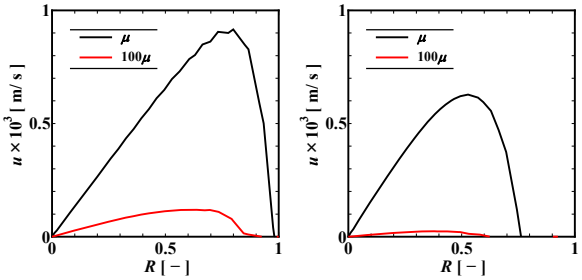

(a) V/V_0= 0.6579 (b) V/V_0= 0.2460

Fig. 9 Outward flow within the droplet.

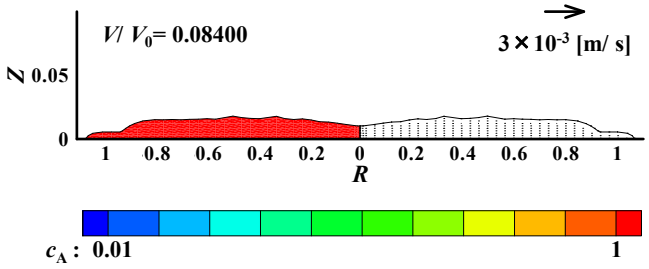

Fig. 10 Thin film configuration from high viscous fluid

CONCLUSION

A mathematical model is proposed to describe the fluid dynamics, mass and heat transfer in a solution droplet evaporating on a flat surface during drying process. A decrease of droplet volume due to evaporation of a solvent, evaporation latent heat generated on the free surface, and an increase of a solute on the free surface are considered in the model. Governing equations are numerical solved using a finite element method. A Lagrangian method is applied to predict the deformation of an evaporating droplet. Firstly, the outward flow caused during self-pinning of the contact line are examined under an ideal condition. The calculated velocity agrees well with that calculated using a one-dimensional model. Secondly, the drying process of a polystyrene/anisole solution droplet with the equivalent diameter of 20 μm are estimated. The migration of the solute at the contact line is found to be almost finished by the instant when a thin liquid film with the solute concentration is still low at the center part. As a result, a ring structure develops on the periphery of the dried film. Lastly, the effect of fluid viscosity is investigated. A high viscosity essentially decreases the velocity of the outward flow, resulting in vanishing the ring structure. The effect of viscosity on the configuration of the film agree with empirical results.

ACKNOWLEDGEMENT

This study is partially supported by the Japan Society for the Promotion of Science (JSPS), Grant-in-Aid for Scientific Research (B) No.22360324.

REFERENCES

1 Fischer, B. J., Particle convection in an evaporating colloidal droplet, *Langmuir*, vol. 18, 2002, pp 60-67.
2 Hu, H., Larson, R. G., Analysis of the microfluid flow in an evaporating sessile droplet, *Langmuir*, vol. 21, 2005, pp. 3963-3971.
3 Hu, H., Larson, R. G., Analysis of the Effects of Marangoni Stresses on the Microflow in an Evaporating Sessile Drople, t*Langmuir*, vol. 21, 2005, pp. 3972-3980.
4 Girard, F., Antoni, M., Faure, S., Steinchen, A., Evaporation and Marangoni driven convection in small heated water droplets, *Langmuir*, vol. 22, 2006, pp. 11085-11091.
5 Hu, H., Larson, R. G., Marangoni effect reverses coffee-ring depositions, *J. Phys. Chem. B* , vol. 110, 2006, pp. 7090-7094.
6 Bhardwaj R., Fang, X., Attinger, D., Pattern formation during the evaporation of a colloidal nanoliter drop: a numerical and experimental study, *New. J. Phys.*, 2009, 075020
7 Yoshitake Y., Yasumatsu, S., Kaneda, M., Nakaso, K., Fukai, J., Structure of circulation flows in polymer solution droplets receding on flat surfaces, *Langmuir*, 2010, vol. 26, 3923-3928.
8 Yasumatsu, S. , Nakaso, K., Fukai, J., Marangoni Flows in Polymer Solution Droplets Drying on Heating Surface, *J. Chem. Eng. Japan*, 2012, vol. 45, pp. 128–135.
9 Hu, H. and Larson, R. G., Evaporation of a Sessile Droplet on a Substrate, *J. Phys. Chem.* B, 2002, vol. 106, 1334.
10 Wilke, C. R., Chang, P., Correlation of Diffusion Coefficients in dilute solutions, *AIChE J.*, 1955 vol. 1, pp. 264-270
11 Fukai, J., Shiiba, Y., Yamamoto, T., Miyatake, O., Poulikakos, D., Megaridis, C. M., Zhao, Z., Wetting Effects on the Spreading of a Liquid Droplet Colliding with a Flat Surface - Experiment and Modeling, *Phys. Fluids A*, 1995, vol. 7, 236-247.
12 Deegan, R. D., Bakajin, O., Dupont, T. F., Huber, G., Nagel, S. F., Witten, T. A., Contact line deposits in an evaporating drop, Phys. Rev. E, 2000, vol. 62, 756 -765